ANTIOXIDANTS & REDOX SIGNALING
Volume 26, Number 3, 2017

DOI: 10.1089/ars.2016.6693

Discoveries

FORUM REVIEW ARTICLE

Structure and Activation of Soluble Guanylyl Cyclase, the Nitric Oxide Sensor

William R. Montfort, Jessica A. Wales, and Andrzej Weichsel

Abstract

Significance: Soluble guanylyl/guanylate cyclase (sGC) is the primary receptor for nitric oxide (NO) and is central to the physiology of blood pressure regulation, wound healing, memory formation, and other key physiological activities. sGC is increasingly implicated in disease and is targeted by novel therapeutic compounds. The protein displays a rich evolutionary history and a fascinating signal transduction mechanism, with NO binding to an N-terminal heme-containing domain, which activates the C-terminal cyclase domains.
Recent Advances: Crystal structures of individual sGC domains or their bacterial homologues coupled with small-angle x-ray scattering, electron microscopy, chemical cross-linking, and Förster resonance energy transfer measurements are yielding insight into the overall structure for sGC, which is elongated and likely quite dynamic. Transient kinetic measurements reveal a role for individual domains in lowering NO affinity for heme. New sGC stimulatory drugs are now in the clinic and appear to function through binding near or directly to the sGC heme domain, relieving inhibitory contacts with other domains. New sGC-activating drugs show promise for recovering oxidized sGC in diseases with high inflammation by replacing lost heme.
Critical Issues: Despite the many recent advances, sGC regulation, NO activation, and mechanisms of drug binding remain unclear. Here, we describe the molecular evolution of sGC, new molecular models, and the linked equilibria between sGC NO binding, drug binding, and catalytic activity.
Future Directions: Recent results and ongoing studies lay the foundation for a complete understanding of structure and mechanism, and they open the door for new drug discovery targeting sGC. *Antioxid. Redox Signal*. 26, 107–121.

Keywords: guanylate cyclase, hypertension, stimulator compound, H-NOX domain, coiled-coil domain, molecular evolution

Introduction

NITRIC OXIDE (NO) is a reactive free-radical diatomic molecule that, nonetheless, regulates a remarkable array of physiological processes in animals. Among these are blood pressure regulation, wound healing, memory formation, odor detection, sexual function, and response to infectious disease (44). In higher animals and many insects, NO is produced by a class of enzymes called nitric oxide synthases, which release NO through the oxidation of L-arginine to L-citrulline (52, 105). The primary NO receptor is soluble guanylyl/guanylate cyclase (sGC), a heterodimeric heme protein of ~150 kDa that responds to NO binding by increasing cyclase activity, producing guanosine 3′,5′-cyclic monophosphate (cGMP), and generating a signaling cascade.

Impaired NO signaling can lead to hypertension and atherosclerosis, and it can contribute to heart attack and stroke (8, 17). Targeting of NO signaling has long been a treatment goal for cardiovascular disease, beginning more than 150 years ago with administration of amyl nitrite (10) and nitroglycerin (71) to relieve symptoms of angina pectoris, although the mode by which these compounds act (release of NO) was not discovered until many years later. More recently, sGC has become a primary target for drug discovery (28).

sGC, the focus of this review, is generally composed of two homologous subunits, α and β, with each containing four recognizable domains that share sequence and structural similarity to bacterial proteins. There is a single heme moiety in the heterodimer that is coordinated to a histidine in the N-terminal domain of the β subunit (His 105 in the human protein). During

Department of Chemistry and Biochemistry, University of Arizona, Tucson, Arizona.

signaling, NO binding to heme leads to the formation of a pentacoordinated Fe-NO complex with proximal histidine bond breakage (26, 103, 116) and stimulation of cyclase activity. Despite much study, how NO binding leads to cyclase activation remains poorly understood, although tantalizing new details are emerging. Likewise, new small-molecule stimulators and activators of sGC have been discovered, opening new doors for drug discovery in the treatment of cardiovascular diseases. However, where they bind and how they function remains unclear.

Here, we describe recent studies on sGC with a particular focus on discoveries since 2010 that reveal structure and provide insight into the signal transduction mechanism. Excellent reviews on sGC function (24, 36), physiology (12, 77), and drug targeting (28, 30) have recently appeared, and they provide summaries of earlier studies and topics beyond the scope of the present review. We refer the reader to these articles for additional information.

Genes and Domain Structure

Genes

sGC displays a fascinating evolutionary history. Insects, worms, algae, and invertebrates employ sGC, but bacteria, fungi, and higher plants apparently do not (29, 91). All sGC proteins are dimeric since the active site forms at the interface of two catalytic domains, one from each subunit. Each sGC subunit is composed of four recognizable domains—a heme domain, a Per-ARNT-Sim (PAS) domain, a coiled-coil signaling helix, and a cyclase domain—that are fused together into a single polypeptide chain of 600–700 amino acids (Fig. 1). Each sGC domain has a bacterial homologue, but the intact sGC gene is more recent. Certain insect and all vertebrate sGC proteins contain one β chain and one α chain in which the ability to bind heme has been lost. Two potential catalytic sites have been reduced to one functional site that utilizes residues from both subunits. Although the other pseudosymmetric site is non-catalytic, it may still bind ligands and serve a regulatory function.

sGC may have first arisen in green algae. For example, the unicellular flagellate *Chlamydomonas reinhardtii*, a well-studied model organism, contains at least three genes coding for possible sGC proteins, CYG12, CYG15, and CYG56. These genes vary considerably in length—coding for proteins of 991, 619, and 1721 amino acids—but each contains all of the expected sGC functional domains. All three have higher similarity with the β chain of vertebrate sGC than with the α chain, and all have the residues needed for forming a functional homodimeric cyclase. That these proteins can, in fact, form functional homodimers has been demonstrated through bacterial expression of the cyclase domains of both CYG12 (119) and CYG56 (20). Thus, sGC appears to have begun as a homodimeric protein.

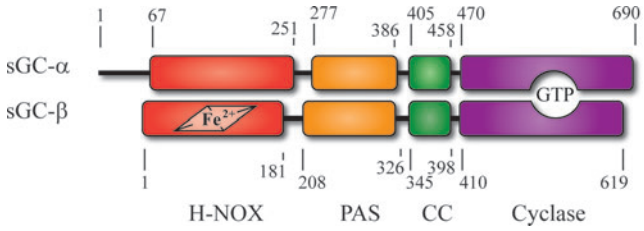

FIG. 1. sGC domain structure. Shown are the approximate boundaries for each domain in sGC. Numbering is for the α1 and β1 subunits of human sGC. sGC, soluble guanylyl/guanylate cyclase. To see this illustration in color, the reader is referred to the web version of this article at www.liebertpub.com/ars

In *Caenorhabditis elegans* (worm), there were a series of gene duplications yielding seven β-subunit-like genes, all of which appear to retain heme domains. These, too, vary in length, particularly at the C-terminus. Although not well characterized, the *C. elegans* sGC proteins appear to be oxygen sensors rather than NO sensors and to function in worm neurons to detect and avoid environments that are too rich or too poor in oxygen (79, 128). Most, but not all, of the residues that are considered to be necessary for homodimeric activity are intact in these genes, suggesting that the corresponding proteins may also function as homodimers. However, genetic knockout studies indicate that they may function in heterodimeric pairs.

Gene duplication to yield the sGC α subunit and α/β heterodimer was well established once insects crawled into existence, and many examples of such proteins are known. We have characterized an α/β sGC from *Manduca sexta*, the hawkmoth, where the protein is required for odor detection and neural activity (18, 40, 72). *Manduca* sGC behaves much like vertebrate $\alpha1/\beta1$ sGC and is considered an $\alpha1/\beta1$ homologue (32, 33, 41, 42, 80, 81). Atypical sGC proteins are also abundant in insects. These proteins are similar to the typical β subunit but may have lost heme binding and appear to function as homodimers (67).

In vertebrates, both the α and β subunits have been duplicated, yielding subunits $\alpha1$, $\alpha2$, $\beta1$, and $\beta2$ (24). The $\alpha1/\beta1$ heterodimer is equivalent to the insect α/β dimer and is widely expressed in mammalian tissues. The $\alpha1/\beta1$ heterodimer is the most thoroughly studied of the sGC proteins and is the primary focus of this review. An $\alpha2/\beta1$ heterodimer is prevalent in nerve cells, but a role for the $\beta2$ subunit has yet to be reported, although it retains all of the residues needed for cyclase activity and may function as a homodimer. Alternative splice variants for the human protein have also been detected (60, 96). These are described in more detail elsewhere in this Forum.

Heme-binding domain

A ferrous *b*-type heme resides in the N-terminal domain of the β subunit and is coordinated through a histidine residue, His 105 in $\alpha1/\beta1$ heterodimers (Fig. 2). This domain was first identified as a ''Heme NO Binding'' domain (45), or an HNOB domain, and this nomenclature persists throughout most sequence databases. Bacterial homologues of the HNOB domain were later discovered to bind oxygen as well as NO, leading to the suggested change in name to H-NOX for heme-nitric oxide oxygen binding (78). H-NOX is the most common name in the literature and is used here. Sensor of nitric oxide (SONO) has been suggested for the domain (73) and is also still in use.

The $\alpha1$ subunit has an extra $\sim$65-residue N-terminal extension that is predicted to be intrinsically disordered. No function has been assigned to these residues, although one report indicates that Ser 64 of the human protein may be a target for phosphorylation by protein kinase G (PKG), which is stimulated by cGMP, leading to feedback inhibition (127).

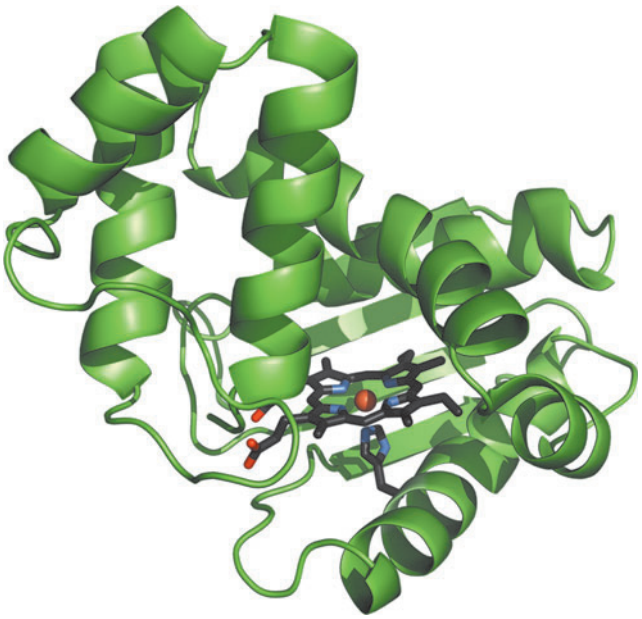

FIG. 2. Homology model for the β1 H-NOX domain. Shown is a ribbon drawing for the heme-binding H-NOX domain in *Ms* sGC (33). Heme and proximal His 105 are shown in stick representations. Carbons are shown in *black*, nitrogens in *blue*, and oxygens in *red*. The helix suggested to be part of signal transduction on NO binding contains His 105 and is at the *bottom* of the figure. Figures 2–7 were prepared with PyMOL (pymol.org). H-NOX, heme-nitric oxide/oxygen binding domain; *Ms* sGC, *Manduca sexta* sGC; NO, nitric oxide. To see this illustration in color, the reader is referred to the web version of this article at www.liebertpub.com/ars

Removal of this domain from *Manduca* sGC leads to greater stability in recombinantly expressed proteins but has little other consequence (42).

Following this N-terminal string of residues of the α subunit is an ''H-NOX'' domain that has lost the ability to bind heme and is thus perhaps best referred to as a pseudo-H-NOX domain. This is the least conserved portion of α1/β1 sGC but, nonetheless, appears to have a regulatory role in signal transduction and also appears to retain an H-NOX fold (42). Removal of this domain in recombinant *Manduca* sGC leads to enhanced CO, and presumably NO, binding to heme (80). Interestingly, one of the splice variants for human α1/β1 sGC is missing this domain (96), which may affect its cellular location (50).

PAS domain

Following the H-NOX domain is a short linker and a PAS domain (also called HNOBA in sGC for HNOB-associated domain). The linker length is conserved in the α1/β1 heterodimeric sGC proteins, but it is quite variable in many β-only sGC proteins. The role of the PAS domain in sGC function is unclear but may enhance dimer formation (55), dampen NO affinity to heme (33), and/or participate in heat shock protein 90 (hsp90)-assisted heme insertion into the β subunit (90).

PAS domains are common in nature and are found both as stand-alone proteins and as components in multi-domain signaling proteins (65). Many PAS domains bind ligands or cofactors such as heme or photoactivatable chromophores and are involved in sensing and signal transduction. Some are connected to coiled-coil signaling helices much like the arrangement in sGC. The first crystal structure for an sGC-related PAS domain was for a domain from a *Nostoc punctiforme* signal transduction histidine kinase (STHK), which revealed a typical PAS domain fold and a potential dimer interface, but no ligand-binding pocket (55). Notably, this domain is attached to a putative coiled-coil signaling helix (55), much like that predicted for sGC, suggesting that an evolutionary link may exist between sGC and more ancient STHK proteins. The crystal structure of the *Manduca* α1 PAS domain displayed a similar fold and a small pocket in the location where ligands often bind to PAS domains (Fig. 3); however, no ligand-binding activity has been discovered for sGC PAS domains.

Coiled-coil domain

Following the PAS domain is a predicted short linker and a coiled-coil domain comprising two helices, one from each subunit. PAS-coiled-coil arrangements are common in signaling proteins, particularly in bacterial STHK proteins such as those from *N. punctiforme*, leading to the suggestion that such domains play a functional role in signal transduction (2). Coiled-coil helices have a characteristic amphipathicity with a solvent-exposed hydrophilic face and a hydrophobic face buried in the coiled-coil interface. Generally, there is a repeating heptad motif (two turns of an α helix) in which bulky

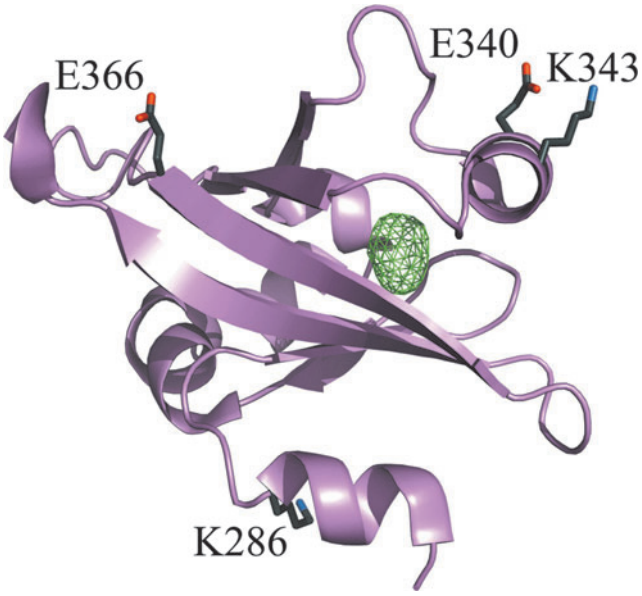

FIG. 3. Crystal structure of the *Ms* sGC α1 PAS domain. Ribbon drawing from PDB file 4GJ4 (81). A small pocket in the protein interior, located where ligands often bind in PAS domain proteins, is shown as a *green cage*. Also shown are residues Glu 340 and Lys 343, which can be cross-linked to the β1 H-NOX domain; residue Lys 286, which can be cross-linked to the β1 PAS domain; and residue Glu 366, which can be cross-linked to the β1 coiled-coil domain. PAS domain, Per-ARNT-Sim domain. To see this illustration in color, the reader is referred to the web version of this article at www.liebertpub.com/ars

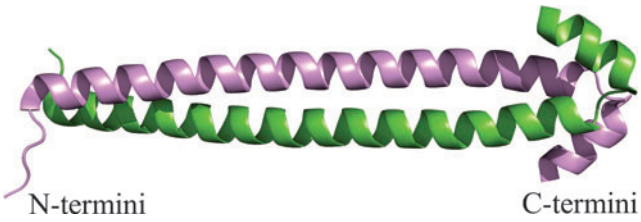

FIG. 4. Model for the α1/β1 coiled-coil domain. A homology model for the α1/β1 *M. sexta* coiled-coil domain (33) is shown as a ribbon drawing with the α chain in *violet* and the β chain in *green*. To see this illustration in color, the reader is referred to the web version of this article at www.liebertpub.com/ars

hydrophobic residues such as leucine and isoleucine appear at the ''a'' and ''d'' positions of the heptad of each helix, allowing for excellent ''knobs-in-holes'' packing at the coiled-coil interface (2). The external surfaces are often charged, and electrostatic interactions may be important for proper coiled-coil formation and alignment.

In α1/β1 sGC, the predicted coiled-coil region is ~50 amino acids long and capped on each end by one or more prolines. Coiled-coil helices can have either parallel or antiparallel chains and the correct orientation can be difficult to predict based on sequence alignment alone, due to the repetitive nature of the heptad repeat. A crystal structure of the rat β1 sGC coiled-coil strand revealed a homodimeric coiled coil in an antiparallel arrangement (54). The authors argued that this was likely an artifact based on electrostatic considerations and that the α1/β1 heterodimeric coiled coil was likely parallel (54). This conclusion was later confirmed by chemical cross-linking analyses that identified cross-links that were only consistent with parallel helices (33). A model for the α1/β1 coiled coil is shown in Figure 4.

Cyclase domains

Signaling through formation of cyclic nucleotides is found in all kingdoms of life and includes not only cAMP and cGMP formation but also formation of the cyclic dinucleotides c-di-GMP and c-di-AMP (37). Cyclic AMP formation occurs in all life forms, whereas cGMP formation is common in animals but is more sporadic in lower eukaryotes, plants, and bacteria.

The sGC cyclase domains are members of the class III cyclase family, the largest cyclase family, and each contains a cyclase homology domain (CHD) (100). The active site in class III cyclases forms at the interface of two CHDs, which can either reside in a single polypeptide or come together through homodimerization or heterodimerization, the arrangement found in α1/β1 sGC. This dimeric arrangement leads to two potential active sites; however, in most cyclases containing two different CHDs, only one of the possible active sites remains catalytically active (Fig. 5). Despite loss of catalytic residues, the other ''pseudosymmetric'' site may retain a functional binding pocket that binds regulatory ligands. For example, forskolin, a natural product that stimulates cAMP production, binds to the pseudosymmetric site of adenylyl cyclase (107, 125).

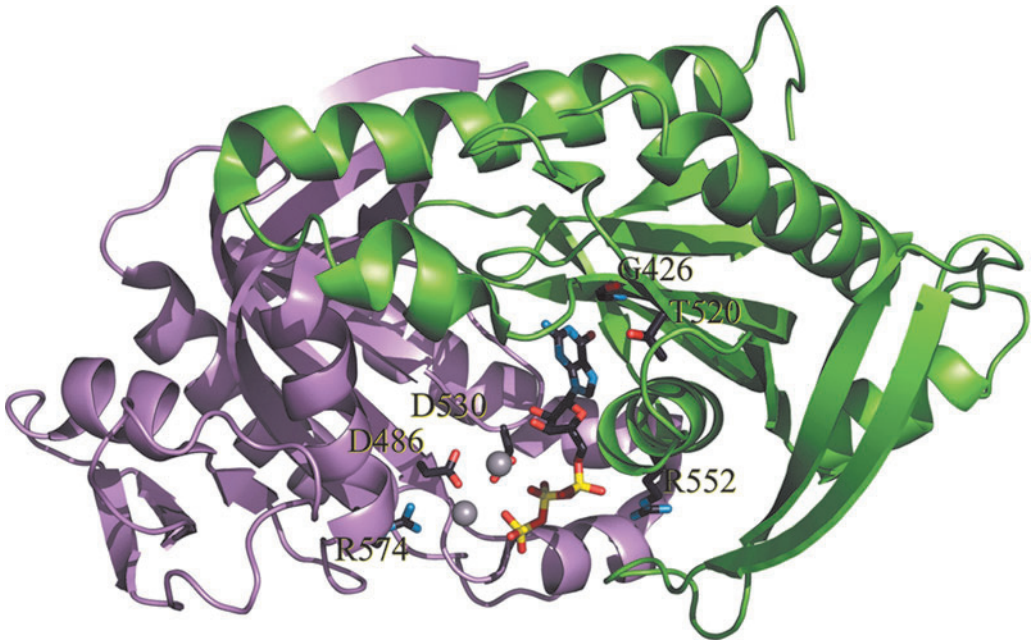

FIG. 5. Model for human cyclase domain with bound GTP. A model for the human cyclase domain with bound GTP was produced by using PDB file 3UVJ (1) and modeling onto a structure of adenylyl cyclase with bound nucleotide, 3MAA (69). A ribbon drawing of the α1 chain is shown in *violet* and the β1 chain is shown in *green*. Also included are catalytic pocket residues Asp 486, Asp 530, and Arg 574 of the α1 chain, Arg 552 of the β1 chain, and GTP as stick drawings. Two magnesium ions required for binding and catalysis are shown as *gray* spheres. β1 Gly 426 and Thr 520, shown in the pseudosymmetric pocket, are equivalent to Asp 486 and Arg 574 of the α1 chain; their change to glycine and threonine contributes to loss of activity for the pseudosymmetric pocket. The overall view is of the ''ventral'' side of the domains, the opposite of the side connecting to the coiled-coil helices. To see this illustration in color, the reader is referred to the web version of this article at www.liebertpub.com/ars

Several crystal structures of adenylyl cyclase domains with bound ligands are known and have led to a model for cyclase domain catalysis in which the ribose 3′ hydroxyl performs an in-line nucleophilic attack on the 5′ α phosphate, leading to pyrophosphate displacement and release (39, 100). Two metal ions are required for the reaction, which can be either Mg^{2+} or Mn^{2+}, with Mg^{2+} being of greater importance *in vivo*.

Two crystal structures of heterodimeric α1/β1 sGC cyclase domains have been reported (1, 94), but, unfortunately, neither structure includes ligands. The overall fold in both structures is similar to that of adenylyl cyclase, with the exception of a small change in the dimer interface that leaves the active site misaligned for efficient catalysis. Catalytic activity for the truncated cyclase domains is quite low, consistent with misalignment of the individual domains, leading to the suggestion that small changes in the H-NOX, coiled-coil, or PAS domains might have large effects on catalytic rates (94). Interestingly, the N-terminal ''dorsal'' face of the cyclase, which is away from the catalytic pocket, is highly conserved in α1/β1 sGC and may provide a functionally important interface with other domains (94). The pseudosymmetric site is collapsed in the cyclase crystal structures and is not capable of binding a ligand the size of forskolin, even after realignment to accommodate GTP binding (1). This site has been suggested as a binding site for ATP (106), which acts as an inhibitor of sGC and appears to have a distinct allosteric binding site (14, 23, 88, 106). For ATP to bind to the pseudosymmetric site, however, additional rearrangement of the domain interface would be needed.

Signal Transduction

Although considerable information is available on sGC domain structure, how these domains are arranged to yield a sensing and signaling unit is much less clear. Binding of NO to the heme domain leads to a signaling cascade that ultimately increases the catalytic rate by as much as 200 fold. NO binding both lowers K_m for GTP and increases k_{cat} (16, 21, 47, 82, 95). A hallmark of NO binding is the release of the proximal histidine from heme coordination, yielding a five-coordinate nitrosyl species, but whether histidine release is simply correlated with activation or is the leading edge of the signaling cascade remains unknown. CO binding, which leads to a six-coordinate species with proximal histidine attached, can also fully activate sGC, but only in the presence of sGC-stimulating compounds, suggesting that proximal histidine breakage is not required for full sGC activity. Additionally, it remains unclear as to how many NO molecules are required for full stimulation, with some data indicating that two or more molecules are required (106). Other complications include the potential roles for nucleotide-based allostery and post-translational modifications.

In this section, we review recent data that are beginning to unravel the domain arrangement in sGC and the signal transduction mechanism. Taken together, these data lead to two models for signal transduction. The first is a model in which the β1 H-NOX domain inhibits the cyclase domain through direct contact. The second is a model in which signaling is transduced from the β1 H-NOX domain through the coiled coil, leading to cyclase domain rearrangement and catalytic activation.

Domain arrangement

Our group uncovered domain–domain contacts among the H-NOX, PAS, and coiled-coil domains by using chemical cross-linking of a truncated form of *M. sexta* sGC lacking the cyclase domains, referred to as *Ms* sGC-NT (33). In this study, amine–amine and amine–carboxylate chemical cross-links were introduced into the recombinant protein, and they were identified by high-resolution tandem mass spectrometry. Both inter-subunit and intra-subunit cross links were identified in this way. The first major conclusion from these data was that the coiled-coil domain was indeed formed from parallel helices, as predicted based on electrostatic considerations (54). The second major conclusion was that the α1 H-NOX and PAS domains were in contact with the β1 H-NOX domain, and that all of these domains appeared to assemble onto the coiled-coil domain (Fig. 6).

We obtained a molecular envelope for *Ms* sGC-NT by using small-angle X-ray scattering (SAXS) and analytical ultracentrifugation (AUC), revealing an elongated molecule with approximate dimensions of 115×90×75 Å. The scattering profiles in these experiments indicated that *Ms* sGC-NT was well folded but exhibited some flexibility. Little change was observed in this envelope on addition of NO, CO, or stimulator compounds, suggesting that the conformational changes that occur on ligand binding are small (on the order

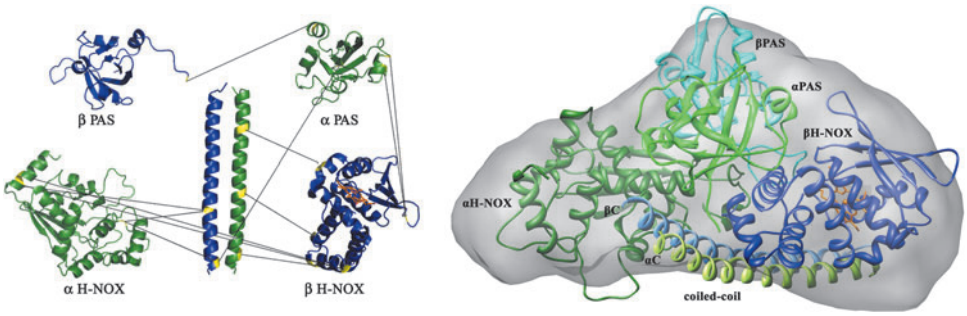

FIG. 6. Model for *Ms* sGC-NT derived from chemical cross-linking, SAXS, and homology modeling. *Left*: Shown are homology models for each domain and intermolecular cross-links between *Ms* sGC-NT α1 and β1 subunits. Cross-links within the coiled coil have been omitted for clarity. *Right*: Energy-minimized model for *Ms* sGC-NT fit to a SAXS molecular envelope. The minimization procedure restrained cross-linked residues to be within cross-linking distance. This figure was assembled from those previously published in Fritz *et al.* (33), with permission. SAXS, small-angle X-ray scattering. To see this illustration in color, the reader is referred to the web version of this article at www.liebertpub.com/ars

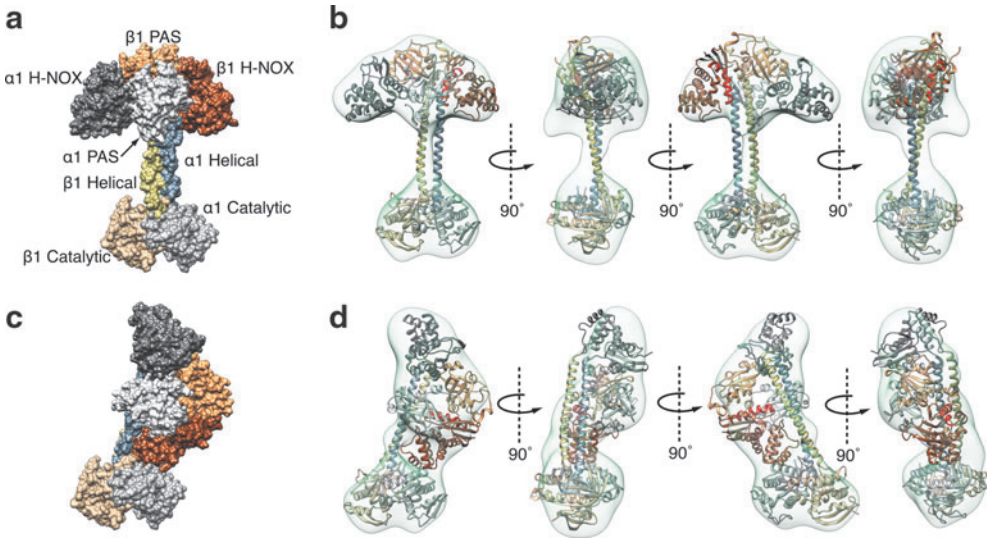

FIG. 7. Models for full-length rat sGC from single-particle electron microscopy. Shown are homology models of individual domains fit into representative electron microscopy maps exhibiting two conformational extremes. **(a, b)** The extended conformation in space-filling and ribbon representations. **(c, d)** The bent conformation with direct contact between the H-NOX/PAS cluster and the parallel coiled-coil domain as well as contact between the β1 H-NOX domain and the α1 cyclase domain. Reprinted from Campbell *et al.* (13), with permission. To see this illustration in color, the reader is referred to the web version of this article at www.liebertpub.com/ars

of a few angstroms) for the truncated protein. We constructed an energy-minimized molecular model by using homology models for each domain and distance restraints from the cross-linking and SAXS data. The resulting model had the coiled coil parallel to the long axis of the molecular envelope with the other domains assembled, on average, onto one coiled-coil face (Fig. 6). The other coiled-coil face was open, providing a potential site for the cyclase domains.

Campbell *et al.* generated a molecular model for the full-length protein from rat by using negative-stain single-particle electron microscopy (13). Their images indicate that sGC may exhibit a wide range of conformations (Fig. 7). The α1/β1 H-NOX and PAS domains occupy an elongated envelope similar to that derived from SAXS analysis. However, these domains appear to occupy multiple orientations with respect to the coiled-coil domain. In some images, they lie alongside of the coiled coil, similar to the SAXS model arrangement, but in other images they appear perpendicular to the coiled-coil domain (Fig. 7). The cyclase domains appear at the opposite end of the coiled coil and perpendicular to the helix axis. A similar distribution of conformations was observed in both the presence and the absence of NO binding or on binding of a non-hydrolyzable GTP analog.

Full models were constructed by using the molecular envelopes provided by electron microscopy (EM), homology models for each domain, and the constraints provided by the previously published cross-linking data. In their modeling, the authors assumed that not all cross-links need to occur at the same time; rather, they are derived from all conformations. In some of the resulting models, the β1 H-NOX is in direct contact with the cyclase domain, where it might directly inhibit cyclase activity, but in others there is no contact. Thus, the models rule out neither proposed activation mechanism–release of direct H-NOX inhibition of cyclase or indirect domain rearrangement.

In a third approach, Behrends and colleagues used Förster resonance energy transfer (FRET) to examine domain proximities. In one experiment, yellow fluorescent protein (YFP) and cyan fluorescent protein (CFP) were fused onto the N- and C-termini of α1/β1 human sGC in various combinations, and FRET efficiency was measured. The data indicated efficient energy transfer between a construct with YFP fused to the α1 C-terminus and CFP fused to the β1 N-terminus (α1-YFP/CFP-β1), leading the authors to conclude that the β1 H-NOX and α1 cyclase are near one another (38). In a second approach, FRET was measured between endogenous tryptophan residues and a fluorescent GTP analog (11). In these studies, NO binding induced enhanced FRET between the fluorescent GTP analog in the active site and a tryptophan residue in the β1 H-NOX domain, or between the fluorescent GTP and a tryptophan in the linker connecting the α1 coiled-coil domain and the α1 cyclase domain. The authors conclude that the β1 H-NOX and the coiled coil are near the cyclase domains and that NO-induced movements force the catalytic domains into the active conformation. These data are more consistent with a compact sGC conformation than with a more extended conformation, and with relatively small NO-induced conformational changes taking place.

Underbakke *et al.* used hydrogen–deuterium exchange mass spectrometry to assess domain interfaces and to identify residues with altered solvent exposure on NO binding (112, 113). Major changes in hydrogen–deuterium exchange rates were found for the β1 H-NOX domain and the cyclase domain on NO binding to full-length rat sGC, as expected. These changes included the H-NOX F-helix, which contains proximal His 105, and active site catalytic residues α1 Asp 485 and α1 Asp 529 (rat numbering). Interestingly, substantial changes were also observed for the coiled-coil helix domain and for the highly conserved N-terminal dorsal face of

the catalytic domains, suggesting that signal transduction may proceed through these regions of the protein. However, the authors conclude that these data do not rule out either of the primary models for NO stimulation: relieving of a direct inhibitory interface between H-NOX and cyclase domains, or rearrangement of the cyclase domains to the active conformation through changes in the coiled-coil domain.

Taken together, these data indicate that sGC forms a compact signaling complex containing H-NOX and PAS domains, a long coiled-coil domain with parallel helices, and a compact cyclase domain. The functional arrangement of these three regions remains unclear, as do the magnitudes of NO-induced conformation changes. Most techniques employed so far suggest that NO-induced changes in conformation are small in scale. However, images using electron microscopy clearly show that large changes in sGC conformation can occur. Caveats exist with all of the experiments addressing domain arrangement and dynamics. Studies with truncated *Ms* sGC-NT are lacking the cyclase domains, which may influence dynamical behavior. The SAXS and AUC analyses are low-resolution techniques and reveal an average conformation. Multiple coiled-coil orientations might not be readily detected by these approaches, since the coiled coil contributes only $\sim$11% of the total *Ms* sGC-NT mass. The electron microscopy is of sGC coated with uranyl formate and dried, which could be harsh. The full-length recombinant protein samples used likely contain a mixture of heme-loaded and heme-free (apo) proteins, based on the ratio of absorbances at 430 nm (heme Soret) and 280 nm (measuring protein) generally reported, which could also affect conformational mobility. The A_{430}/A_{280} should be $\sim$1 for the full-length protein (27, 62) but is often much less than 1 for the recombinant proteins.

Of the models most commonly presented, we favor one in which signal transduction occurs through NO-induced changes in the coiled-coil helices. Such a model would allow signal transduction in a compact or an extended domain arrangement, and in a static or highly flexible molecule, as implied by the SAXS and EM data. In support of this model, small changes in coiled-coil length yield large changes in ligand affinity (described later) whereas ligand binding results in little change to SAXS and AUC molecular envelopes for *Ms* sGC-NT, or conformation distribution for full-length sGC as seen by EM.

Coiled-coil helices are increasingly discovered to play an active role in signal transduction and for this reason are sometimes referred to as signaling helices. Despite their widespread occurrence, the underlying mechanisms governing signal transduction through signaling helices are largely unknown (2). Signaling through coiled-coil helices has precedent in bacterial two-component systems, from which the sGC PAS-coiled-coil arrangement likely evolved, and in related bacterial proteins. One example is the sensor histidine kinase YF1, which appears to signal *via* a change in coiled-coil helix cross-over angle (25). A second example is for the transcriptional regulator DhaR, which appears to signal through a rotation of coiled-coil helices (98). In both examples, activation occurs through small changes in domain orientation rather than through large structural rearrangements. These data make clear that signal transduction through the coiled coil is a viable possibility for sGC. Determination of whether it is the correct mechanism awaits the results of high-resolution structural studies.

Linked equilibria

It has long been known that NO binding to the heme in sGC enhances GTP affinity for the cyclase domain, leading to a lower K_m value (114). NO also enhances binding of other nucleotides, including product cGMP, which leads to increased product inhibition (57). The reverse should also be true, but the demonstration of enhanced NO binding in the presence of nucleotide has been more challenging to directly demonstrate due to the complicated nature of NO binding. One challenge is the very high affinity of NO for heme after proximal histidine release (87, 110). A second is the possibility that multiple NO binding sites reside in the protein (14, 110). Another complication is an apparent second binding site for nucleotides, which induce additional allosteric regulation (14, 16, 88, 106, 121). Nucleotide binding clearly changes NO-binding behavior, but precisely how remains unclear. Published conclusions are influenced by the time scale of measurement, which spans picoseconds to seconds, and the concentration of NO used, which is often in the micromolar range, yielding a robust signal, whereas binding affinity is in the nanomolar to picomolar range. These factors paired with the inherent reactivity of NO make key NO binding and release measurements difficult to acquire, and data interpretation challenging and controversial (14, 87, 89, 110).

Despite these challenges, recent studies make it clear that individual sGC regulatory domains modulate heme affinity for distal pocket ligands such as NO and CO. The inherent affinity of the β1 H-NOX domain for CO, and presumably NO, is high in the absence of other domains, displaying a value as low as $K_d = 200$ n*M* for *Ms* sGC (80). Binding affinity is reduced as additional domains are included: CO-binding affinity decreases $\sim$10 fold for an *Ms* sGC construct containing the α1 PAS and coiled-coil domains, and $\sim$250 fold for an *Ms* sGC-NT construct possessing an intact α1 H-NOX domain in addition to the α1 PAS and coiled-coil domains (80). A similar trend is observed with bovine sGC, although CO binding to the bovine protein is, in general, weaker than to the *Manduca* protein (80). Much of the increased affinity derives from an enhanced on rate for bimolecular binding to the isolated heme domain and an increased rebinding (geminate binding phase) on dissociation (122).

Taken together, these data suggest that the other domains in sGC either induce a strained heme geometry that binds gaseous ligands less well or induce an open heme pocket that facilitates ligand escape. Addition of allosteric stimulators such as nucleotides or stimulating compounds such as YC-1 (described in a later section) relieve this strain or close the heme pocket, allowing for tighter binding of NO and CO.

Coiled-coil domain influence on NO binding

Kinetic measurements also provide insight into the mechanism behind sGC signal transduction, particularly with respect to the coiled-coil domain. In stopped-flow kinetic measurements with full-length sGC, the transient six-coordinate NO complex can be detected and the rate of its decay to a five-coordinate species can be measured, leading to a rate constant of $\sim 10\ s^{-1}$, depending on temperature, NO concentration, and other experimental variables (110, 123, 126). For the β1 H-NOX alone, decay of the six-coordinate intermediate is accelerated and too fast to be observed in rapid-mixing experiments (126). Interestingly, truncated

versions of *Ms* sGC containing the full coiled-coil domain also display slow proximal His 105 release, again with a rate constant of $\sim 10\,s^{-1}$ (42). However, a 10-residue truncation of the coiled coil speeds up proximal His 105 cleavage to $>100\,s^{-1}$ such that it can no longer be observed by stopped-flow spectrophotometry (33). These data are consistent with signal transduction occurring through coiled-coil rearrangement, such as occurs in the bacterial two-component systems discussed earlier.

Heme Domain Properties

Trapping gas with ferrous heme

Ferrous [Fe(II)] heme can bind to numerous gaseous ligands, including O_2, CO, and NO. Oxidation to ferric [Fe(III)] heme leads to loss of O_2 and CO binding, and to reduced NO-binding affinity. Globins use ferrous *b*-type heme for O_2 transport and storage, whereas the nitrophorins use ferric *b*-type heme for NO transport and storage during feeding by certain bloodsucking insects (66, 83, 115, 117, 118). A hallmark of sGC is the use of ferrous *b*-type heme to tightly bind NO but discriminate against O_2, which could lead to an unwanted reaction with NO in the heme pocket. Oxygen binding to sGC has been described, but only at a temperature of 77 K, and only yielding partial saturation in the absence of stimulating compounds (56).

Two factors are likely responsible for the low oxygen affinity of sGC heme. First, oxygen binding is inherently weak to ferrous heme. For example, oxygen binding to an imidazole-capped model small-molecule heme displays $K_d = 5\,\mu M$ (15), a value about 10^3 fold larger than for CO binding, and 10^6 fold larger than for NO binding (86). In myoglobin, O_2 binding is improved about 100 fold through hydrogen bonding to the distal-pocket histidine [reviewed in Ref. (109)], but no such group exists in sGC. *Tt* H-NOX, however, does bind O_2 and binding is stabilized through a distal-pocket tyrosine (78). Introduction of a distal-pocket tyrosine into sGC led to mixed results, with binding apparently occurring for the isolated H-NOX domain but not in the full-length protein (9, 22, 58). However, oxygen binding could be detected in full-length sGC on addition of a second distal-pocket mutation in a position suggested by homology modeling of the *Drosophila* sGC Gyc-88E, an atypical sGC that does bind oxygen (22). Thus, the absence of an appropriate hydrogen-bond donating group likely contributes to the lack of oxygen binding in the wild-type protein.

The second factor limiting oxygen binding is an overall decreased affinity for all gaseous ligands through changes in the heme pocket or heme geometry. Tsai *et al.* have proposed a ''sliding scale rule'' for ferroheme proteins such that the affinity ratios of O_2:CO:NO are always about $1:10^3:10^6$ for imidazole-coordinated heme (109, 111). Using the sliding scale model, Tsai *et al.* predict binding of O_2 to full-length human sGC to have $K_d = \sim 1\,M$. Since the concentration of O_2 in air-saturated solutions at room temperature and atmospheric pressure is $\sim 250\,\mu M$, significant binding should not occur and, indeed, binding is not seen even in fully oxygenated solutions (102).

As previously noted, one likely role of the other sGC domains is to modulate the H-NOX domain affinity for NO and other gaseous ligands, including O_2, leading to overall lower affinity for all ligands (80, 122). For example, the inherent CO affinity for the β chain H-NOX domain is much higher when isolated than when placed in the full-length protein (80). Importantly, although O_2, CO, and NO have lower affinity to six-coordinate full-length sGC than to other ferroheme proteins, NO binding leads to proximal histidine release and an $\sim 10^4$-fold increase in NO affinity, resulting in picomolar K_d values. This high-affinity state for NO appears to be disproportionately enhanced through a change in conformation that stabilizes proximal histidine displacement.

The mechanism behind the overall tuning of gaseous ligand affinity could be through changes in heme geometry, changes in protein conformation that alter the ability for ligands to escape, or a combination of both. Inducing a conformation with heme iron pulled below the heme plane (toward the proximal pocket) would reduce ligand affinity, whereas placing the heme iron into or above the heme plane (toward the distal pocket) would increase ligand affinity. This mechanism is used to alter oxygen affinity in hemoglobin on switching between R and T states. The bacterial H-NOX proteins have decidedly non-planar heme geometries, which lends support to this model, and heme flattening is suggested to be key for signal transduction in these proteins (70). Alternatively, blocking escape from the heme pocket, leading to geminate recombination rather than escape from the protein, could also enhance affinity. This mechanism is used by the nitrophorins, which transport NO and enhance binding at low pH by blocking the distal pocket with two conformationally mobile loops (6, 117). Both binding of compound YC-1 to sGC (41) and removal of the α_1 chain (122) lead to enhanced geminate recombination, but whether this is due to a change in heme geometry, a blocking of ligand escape, or both is yet to be determined.

Reduction potential

sGC is designed to function as a ferrous heme protein, which allows it to sense very low NO concentrations, in the picomolar range (4, 120). At these concentrations, NO side reactions are minimized and sGC becomes the primary NO receptor. Ferric heme can also bind NO, but binding affinity drops to the nanomolar to micromolar range (108). To preserve picomolar NO affinity, the sGC heme is highly stabilized in the ferrous state, considerably more so than the same heme in hemoglobin or myoglobin. The midpoint potential measured for truncated *Manduca* sGC was +234 mV (32), whereas that for the full-length bovine protein was measured as +187 mV (56). The midpoint potential for the bacterial *Tt* H-NOX was measured as +167 mV, indicating that the stabilized ferrous state for this domain is highly conserved.

Heme reduction potentials are set by the binding pocket in heme proteins and can vary by nearly a volt overall. How this is accomplished remains incompletely understood, but two factors have been investigated. First, the electrostatic environment is important, with ferric heme, having a formal charge of +1, often stabilized through nearby negative charges. For example, the *Rhodnius* nitrophorins, which are ferric heme proteins, display a midpoint potential of about −300 mV and have a heme pocket surrounded by numerous Glu and Asp residues. Mutation of these residues shifts the midpoint potential to be more positive (ferrous) (7). H-NOX domains generally have quite hydrophobic heme pockets, which are consistent with stabilizing the ferrous state.

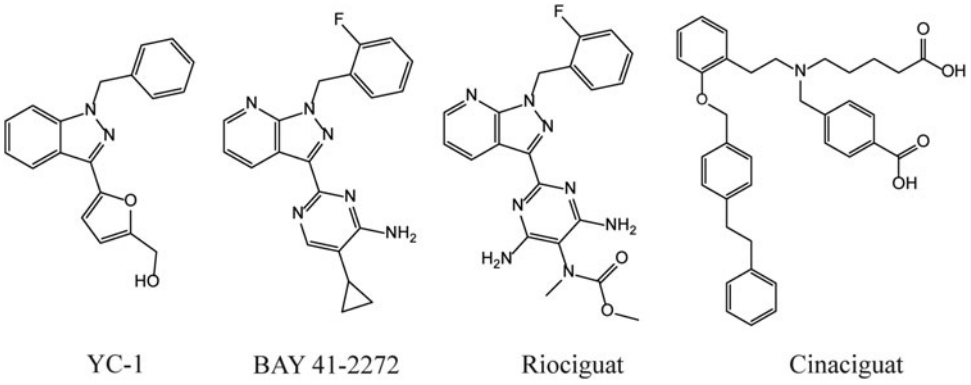

FIG. 8. sGC stimulators and activators. Shown are the structures for sGC stimulators YC-1, BAY 41-2272, and riociguat, which stimulate intact sGC and are synergistic with NO stimulation. Also shown is cinaciguat (BAY 58-2667), which activates heme-depleted sGC.

A second factor considered to influence the midpoint potential is heme planarity. Heme distortion is often conserved in heme proteins and greater distortion, particularly heme ''ruffling,'' has been correlated with more negative (ferric) midpoint potentials (97). The nitrophorins, for example, display among the most distorted protein-bound hemes known (85) and are stabilized in the ferric state (3, 99). However, the bacterial H-NOX proteins also display highly distorted heme geometries but are highly stabilized in the ferrous state, just the opposite of the nitrophorins. Mutations designed to test the role of heme distortion in setting the reduction potential are intriguing but have not resolved the issue. Mutations designed to flatten the nitrophorin heme led to more positive (ferrous) midpoint potentials for the nitrosyl complexes; however, results for the aqua complexes were mixed (99). Mutations that flatten the *Tt* H-NOX heme led to more negative (ferric) midpoint potentials (74, 75), leading the authors to suggest that heme distortion stabilizes the ferrous state, the opposite of that proposed for the nitrophorins. Binding pocket hydrophobicity and heme distortion in sGC are likely to be critical for function; however, understanding how these factors influence the ferrous state remains to be uncovered.

sGC as a Drug Target

Unwittingly, sGC has long been a target for drugs that deliver NO for the treatment of cardiovascular disease, beginning with organic nitrates such as glyceryl trinitrate (nitroglycerin) in the 1860s to treat angina pectoris [reviewed in Ref. (19)]. Organic nitrates, which are metabolized to release NO, remain a staple treatment for relieving the acute symptoms of congestive heart failure, coronary artery disease, and arterial hypertension; however, nitrate tolerance rapidly reduces the effectiveness of these compounds, possibly in part through a mechanism leading to sGC heme oxidation (46).

More recently, compounds that directly enhance sGC activity have been discovered. The first of these was the compound YC-1 (Fig. 8), a benzylindazole derivative that can inhibit platelet activation through stimulating sGC (49). YC-1 and related compounds stimulate sGC activity two- to fourfold in the absence of NO, but they act synergistically with CO or NO to achieve several hundred-fold activation (31, 104). The compounds require an intact heme for activity and are commonly referred to as sGC *stimulators* [reviewed in Refs. (28, 30)]. YC-1 binding can also overcome inhibitory phosphorylation of sGC (82). YC-1 optimization led to numerous related stimulator compounds, including BAY 41-2272, which has seen extensive use for investigating stimulator mechanism, and compound BAY 63-2521 (riociguat), a YC-1 derivative that has recently completed phase III clinical trials (5, 34, 35, 64) and is now FDA approved for treatment of pulmonary hypertension (marketed as Adempas). However, despite much work, where YC-1 and related stimulator compounds bind to sGC and how they increase catalytic activity remains unknown, although it now appears likely that binding is directly to the β1 H-NOX domain, as discussed next.

A second class of compounds, referred to as sGC *activators*, target heme-depleted sGC, which can occur in response to inflammation and oxidative stress (30). Prominent among these are compounds BAY 58-2667 (cinaciguat, Fig. 8) (93)

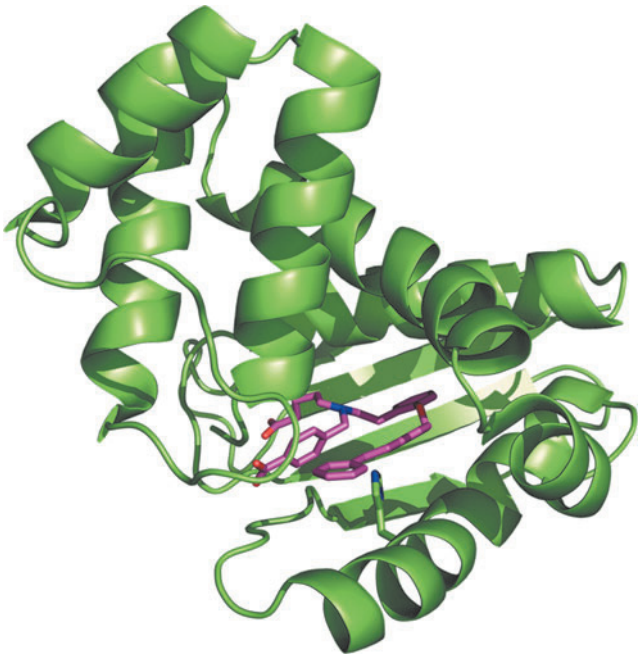

FIG. 9. Bacterial H-NOX in complex with BAY 58-2667 (cinaciguat). Shown is the crystal structure of cinaciguat in complex with *Nostoc* bacterial H-NOX (PDB 3L6J) (61). The protein backbone is illustrated with a ribbon drawing and cinaciguat as sticks. To see this illustration in color, the reader is referred to the web version of this article at www.liebertpub.com/ars

and HMR1766 (ataciguat) (92). Activators are proposed to occupy the heme cavity in sGC after heme oxidation and loss, thereby both stimulating activity and reducing proteasomal degradation (63). A crystal structure of cinaciguat bound to the heme-depleted bacterial *Nostoc* H-NOX domain (61) provides strong evidence in support of this model (Fig. 9). In the structure, cinaciguat occupies the heme pocket and folds into a heme-like conformation with its two carboxylate substituents arranged much like that of the two heme propionates in the native structure. Helix αF, which contains the proximal histidine, occupies a conformation that is considered to occur in NO-activated sGC, which is consistent with cinaciguat acting as an sGC activator.

Although the mechanism underlying activator function seems clear, how stimulator compounds bind to and stimulate sGC remains a mystery. Photoaffinity labeling of rat sGC with a BAY 41-2272 analog revealed cross-links to Cys 238 and Cys 243 in the α1 H-NOX domain (101), suggesting that this domain contains the compound binding pocket, an attractive possibility since homology modeling suggested that a remnant of the heme-binding pocket might be retained in the domain (42). A second attractive possibility is for binding to occur in the pseudosymmetric site of the cyclase domains, much as forskolin binds in adenylyl cyclase (51), and this suggestion remains popular (57, 68, 121) despite strong data indicating that binding occurs elsewhere.

The most compelling data indicate that stimulator compounds bind to the N-terminal portion of the β1 chain, most likely to the H-NOX domain itself. Binding of the compounds to full-length sGC (i) enhances CO binding (48); (ii) leads to greater geminate recombination in photolysis experiments (124); (iii) leads to a small shift in the heme Soret absorption band for the CO complex (48, 124); and (iv) leads to changes in the resonance Raman vibrational spectra (43, 53, 59, 76). Importantly, all four binding indicators occur with full-length sGC as well as with truncated sGC lacking the cyclase domains or the entire α1 subunit. For example:

- Binding of stimulator PF-25 (84) to *Ms* sGC β1 1-380, which contains the β1 H-NOX, PAS, and coiled-coil domains, but lacks both cyclase domains and all of the α1 chain, was directly measured by using surface plasmon resonance (SPR) (80). The measurements revealed PF-25 K_d values of 7 μM (+NO) and 92 μM (–NO).
- CO-binding affinity for an *Ms* sGC-NT construct containing α1 272-450 (PAS-CC) and β1 1-380 (H-NOX-PAS-CC) is enhanced 11 fold by YC-1 and 31 fold by BAY 41-2272 (80), indicating that functional binding does not require the α1 H-NOX domain or either of the cyclase domains.
- Binding of either YC-1 or BAY 41-2272 to CO-ligated *Ms* sGC-NT constructs induces an ~2 nm shift in the Soret band (41, 80), allowing for compound affinity to the CO complexes to be measured *via* compound titration. K_d values for YC-1 ranged between 600 and 800 nM using this approach, depending on construct, and between 80 and 90 nM for BAY 41-2272.
- Binding of YC-1 or BAY 41-2272 to the CO complex of *Clostridium botulinum* H-NOX (*Cb*-SONO) (124) also exhibited a shift in Soret band maximum, suggesting that binding may be conserved in all H-NOX domains.
- Binding of YC-1 or BAY 41-2272 to *Ms* sGC-NT (41), bovine β1 H-NOX (residues 1–200) (124), and *Cb*-SONO (H-NOX) (124) leads to faster rebinding of CO and increased geminate recombination after flash photolysis.
- Resonance Raman spectra for YC-1 ligated protein (CO-complex) are similar for the full-length bovine protein and a construct containing only residues β1 1-385 (H-NOX-PAS-CC) (43).

In contrast, one recent report examined binding of YC-1 and related stimulator compounds to the isolated cyclase domains by SPR, and found binding to occur (68). These measurements were for a single compound concentration (100 μM) and displayed rapid association and dissociation kinetics, which did not allow for affinity constants to be determined. In a separate study, YC-1 was unable to stimulate catalytic activity in the isolated cyclase domains (23), suggesting that the binding to the cyclase domains seen by SPR was non-specific rather than functional, at least for the isolated domains. Despite the possibility that some level of binding may occur in the cyclase domains, overall, the data strongly indicate that functional binding for stimulator compounds is in the H-NOX domain.

Linked equilibria for drug binding

A concern with some of the stimulator binding studies is the high concentration of YC-1 used (as high as 200 μM), which could result in non-specific binding and generate non-specific spectral changes. However, only nanomolar quantities of YC-1 or BAY 41-2272 are needed to induce a shift in the *Ms* sGC-NT-CO Soret absorption band, providing confidence that a specific binding event occurs. We developed a linked-equilibria analysis to extract dissociation constants for both CO and compound binding to *Ms* sGC-NT constructs, as well as the allosteric enhancement factor exerted on one ligand through binding of the other (80). As expected, CO binding led to tighter binding of YC-1 or BAY 41-2272, just as YC-1 or BAY 41-2272 binding led to tighter CO binding. K_d values ranged from 9 to 21 μM for YC-1, and from 2 to 17 μM for BAY 41-2272, depending on the construct used. Cooperativity factors, which measure the degree to which binding of one ligand enhances binding of the other, were ~17 for the weaker binding YC-1, and ~135 for the tighter binding BAY 41-2272. Using similar logic and catalytic rate enhancements, Roy *et al.* extracted dissociation constants for BAY 41-2272 binding to full-length sGC in the presence or absence of NO, which yielded K_d values of 11 μM and 20 nM, respectively (87). Thus, the success of a particular stimulator compound correlates with its ability to induce an sGC conformation with a high affinity for NO, CO, and GTP.

Conclusions

Soluble guanylyl cyclase is a heterodimeric protein comprising α and β chains in animals. Both subunits have four domains, each with bacterial homologues. A crystal structure of the full protein has yet to be obtained but domain arrangement is becoming clear from SAXS, chemical cross-linking, FRET and EM studies. Binding of NO to a ferrous heme in the β subunit increases both active site affinity for substrate GTP and overall catalytic rate. EM studies indicate that sGC is a

flexible molecule, but signal transduction may require only small rearrangements that are transmitted from the heme domain through the coiled coil to the active site, which resides between two cyclase domains and may require only small adjustments for activation or inhibition. A promising family of stimulatory compounds bind near or directly to the heme domain, leading to enhanced affinity for NO and CO, and enhanced catalysis. Open questions include the overall structure of sGC; the signal transduction mechanism; the number of NO molecules needed for full activation; regulation by ATP and other nucleotides; and the role of post-translational modification in sGC function. sGC is a highly sought-after therapeutic target for overcoming cardiovascular disease. Although much has been learned, unlocking the full potential of sGC as a drug target awaits the answers to these questions.

Acknowledgments

This work was supported in part by grants from the National Institutes of Health (R01 GM117357 and P30 CA023074 to W.R.M., and T32 GM008804 to J.W.), the American Heart Association and the AHA Phoenix Heart Ball (14GRNT20080006 to W.R.M.), and a contract from Ironwood Pharmaceuticals (100003104 to W.R.M.). The authors are grateful to Melody Campbell, Bridget Carragher, and Michael Marletta for Figure 7.

References

1. Allerston CK, von Delft F, and Gileadi O. Crystal structures of the catalytic domain of human soluble guanylate cyclase. *PLoS One* 8: e57644, 2013.
2. Anantharaman V, Balaji S, and Aravind L. The signaling helix: a common functional theme in diverse signaling proteins. *Biol Direct* 1: 25, 2006.
3. Andersen JF, Ding XD, Balfour C, Shokhireva TK, Champagne DE, Walker FA, and Montfort WR. Kinetics and equilibria in ligand binding by nitrophorins 1–4: evidence for stabilization of a NO-ferriheme complex through a ligand-induced conformational trap. *Biochemistry* 39: 10118–10131, 2000.
4. Batchelor AM, Bartus K, Reynell C, Constantinou S, Halvey EJ, Held KF, Dostmann WR, Vernon J, and Garthwaite J. Exquisite sensitivity to subsecond, picomolar nitric oxide transients conferred on cells by guanylyl cyclase-coupled receptors. *Proc Natl Acad Sci U S A* 107: 22060–22065, 2010.
5. Belik J. Riociguat, an oral soluble guanylate cyclase stimulator for the treatment of pulmonary hypertension. *Curr Opin Investig Drugs* 10: 971–979, 2009.
6. Benabbas A, Ye X, Kubo M, Zhang Z, Maes EM, Montfort WR, and Champion PM. Ultrafast dynamics of diatomic ligand binding to nitrophorin 4. *J Am Chem Soc* 132: 2811–2820, 2010.
7. Berry RE, Shokhirev MN, Ho AY, Yang F, Shokhireva TK, Zhang H, Weichsel A, Montfort WR, and Walker FA. Effect of mutation of carboxyl side-chain amino acids near the heme on the midpoint potentials and ligand binding constants of nitrophorin 2 and its NO, histamine, and imidazole complexes. *J Am Chem Soc* 131: 2313–2327, 2009.
8. Bian K, Doursout MF, and Murad F. Vascular system: role of nitric oxide in cardiovascular diseases. *J Clin Hypertens (Greenwich)* 10: 304–310, 2008.
9. Boon EM, Huang SH, and Marletta MA. A molecular basis for NO selectivity in soluble guanylate cyclase. *Nat Chem Biol* 1: 53–59, 2005.
10. Brunton TL. Use of nitrite of amyl in angina pectoris. *Lancet* 90: 97–98, 1867.
11. Busker M, Neidhardt I, and Behrends S. Nitric oxide activation of guanylate cyclase pushes the alpha1 signaling helix and the beta1 heme-binding domain closer to the substrate-binding site. *J Biol Chem* 289: 476–484, 2014.
12. Buys E and Sips P. New insights into the role of soluble guanylate cyclase in blood pressure regulation. *Curr Opin Nephrol Hypertens* 23: 135–142, 2014.
13. Campbell MG, Underbakke ES, Potter CS, Carragher B, and Marletta MA. Single-particle EM reveals the higher-order domain architecture of soluble guanylate cyclase. *Proc Natl Acad Sci U S A* 111: 2960–2965, 2014.
14. Cary SP, Winger JA, and Marletta MA. Tonic and acute nitric oxide signaling through soluble guanylate cyclase is mediated by nonheme nitric oxide, ATP, and GTP. *Proc Natl Acad Sci U S A* 102: 13064–13069, 2005.
15. Chang CK and Traylor TG. Reversible oxygenation of protoheme-imidazole complex in aqueous solution (1, 2). *Biochem Biophys Res Commun* 62: 729–735, 1975.
16. Chang FJ, Lemme S, Sun Q, Sunahara RK, and Beuve A. Nitric oxide-dependent allosteric inhibitory role of a second nucleotide binding site in soluble guanylyl cyclase. *J Biol Chem* 280: 11513–11519, 2005.
17. Coggins MP and Bloch KD. Nitric oxide in the pulmonary vasculature. *Arterioscler Thromb Vasc Biol* 27: 1877–1885, 2007.
18. Collmann C, Carlsson MA, Hansson BS, and Nighorn A. Odorant-evoked nitric oxide signals in the antennal lobe of *Manduca sexta*. *J Neurosci* 24: 6070–6077, 2004.
19. Daiber A and Munzel T. Organic nitrate therapy, nitrate tolerance, and nitrate-induced endothelial dysfunction: emphasis on redox biology and oxidative stress. *Antioxid Redox Signal* 23: 899–942, 2015.
20. de Montaigu A, Sanz-Luque E, Galvan A, and Fernandez E. A soluble guanylate cyclase mediates negative signaling by ammonium on expression of nitrate reductase in *Chlamydomonas*. *Plant Cell* 22: 1532–1548, 2010.
21. Denninger JW, Schelvis JPM, Brandish PE, Zhao Y, Babcock GT, and Marletta MA. Interaction of soluble guanylate cyclase with YC-1: kinetic and resonance Raman studies. *Biochemistry* 39: 4191–4198, 2000.
22. Derbyshire ER, Deng S, and Marletta MA. Incorporation of tyrosine and glutamine residues into the soluble guanylate cyclase heme distal pocket alters NO and O2 binding. *J Biol Chem* 285: 17471–17478, 2010.
23. Derbyshire ER, Fernhoff NB, Deng S, and Marletta MA. Nucleotide regulation of soluble guanylate cyclase substrate specificity. *Biochemistry* 48: 7519–7524, 2009.
24. Derbyshire ER and Marletta MA. Structure and regulation of soluble guanylate cyclase. *Annu Rev Biochem* 81: 533–559, 2012.
25. Diensthuber RP, Bommer M, Gleichmann T, and Moglich A. Full-length structure of a sensor histidine kinase pinpoints coaxial coiled coils as signal transducers and modulators. *Structure* 21: 1127–1136, 2013.
26. Dierks EA, Hu S, Vogel KM, Yu AE, Spiro TG, and Burstyn JN. Demonstration of the role of scission of the proximal histidine-iron bond in the activation of soluble guanylyl cyclase though metalloporphyrin substitution studies. *J Am Chem Soc* 119: 7316–7323, 1997.

27. Emmons TL, Mathis KJ, Shuck ME, Reitz BA, Curran DF, Walker MC, Leone JW, Day JE, Bienkowski MJ, Fischer HD, and Tomasselli AG. Purification and characterization of recombinant human soluble guanylate cyclase produced from baculovirus-infected insect cells. *Protein Expr Purif* 65: 133–139, 2009.
28. Evgenov OV, Pacher P, Schmidt PM, Hasko G, Schmidt HH, and Stasch JP. NO-independent stimulators and activators of soluble guanylate cyclase: discovery and therapeutic potential. *Nat Rev Drug Discov* 5: 755–768, 2006.
29. Fitzpatrick DA, O'Halloran DM, and Burnell AM. Multiple lineage specific expansions within the guanylyl cyclase gene family. *BMC Evol Biol* 6: 26, 2006.
30. Follmann M, Griebenow N, Hahn MG, Hartung I, Mais FJ, Mittendorf J, Schafer M, Schirok H, Stasch JP, Stoll F, and Straub A. The chemistry and biology of soluble guanylate cyclase stimulators and activators. *Angew Chem Int Ed Engl* 52: 9442–9462, 2013.
31. Friebe A, Schultz G, and Koesling D. Sensitizing soluble guanylyl cyclase to become a highly CO-sensitive enzyme. *EMBO J* 15: 6863–6868, 1996.
32. Fritz BG, Hu X, Brailey JL, Berry RE, Walker FA, and Montfort WR. Oxidation and loss of heme in soluble guanylyl cyclase from *Manduca sexta*. *Biochemistry* 50: 5813–5815, 2011.
33. Fritz BG, Roberts SA, Ahmed A, Breci L, Li W, Weichsel A, Brailey JL, Wysocki VH, Tama F, and Montfort WR. Molecular model of a soluble guanylyl cyclase fragment determined by small-angle X-ray scattering and chemical cross-linking. *Biochemistry* 52: 1568–1582, 2013.
34. Ghofrani HA, D'Armini AM, Grimminger F, Hoeper MM, Jansa P, Kim NH, Mayer E, Simonneau G, Wilkins MR, Fritsch A, Neuser D, Weimann G, and Wang C. Riociguat for the treatment of chronic thromboembolic pulmonary hypertension. *N Engl J Med* 369: 319–329, 2013.
35. Ghofrani HA, Galie N, Grimminger F, Grunig E, Humbert M, Jing ZC, Keogh AM, Langleben D, Kilama MO, Fritsch A, Neuser D, and Rubin LJ. Riociguat for the treatment of pulmonary arterial hypertension. *N Engl J Med* 369: 330–340, 2013.
36. Gileadi O. Structures of soluble guanylate cyclase: implications for regulatory mechanisms and drug development. *Biochem Soc Trans* 42: 108–113, 2014.
37. Gomelsky M. cAMP, c-di-GMP, c-di-AMP and now cGMP: bacteria use them all! *Mol Microbiol* 79: 562–565, 2011.
38. Haase T, Haase N, Kraehling JR, and Behrends S. Fluorescent fusion proteins of soluble guanylyl cyclase indicate proximity of the heme nitric oxide domain and catalytic domain. *PLoS One* 5: e11617, 2010.
39. Hahn DK, Tusell JR, Sprang SR, and Chu X. Catalytic mechanism of mammalian adenylyl cyclase: a computational investigation. *Biochemistry*, 54: 6252–6262, 2015.
40. Higgins M, Miller M, and Nighorn A. Nitric oxide has differential effects on currents in different subsets of *Manduca sexta* antennal lobe neurons. *PLoS One* 7: e42556, 2012.
41. Hu X, Feng C, Hazzard JT, Tollin G, and Montfort WR. Binding of YC-1 or BAY 41-2272 to soluble guanylyl cyclase induces a geminate phase in CO photolysis. *J Am Chem Soc* 130: 15748–15749, 2008.
42. Hu X, Murata LB, Weichsel A, Brailey JL, Roberts SA, Nighorn A, and Montfort WR. Allostery in recombinant soluble guanylyl cyclase from *Manduca sexta*. *J Biol Chem* 283: 20968–20977, 2008.
43. Ibrahim M, Derbyshire ER, Marletta MA, and Spiro TG. Probing soluble guanylate cyclase activation by CO and YC-1 using resonance Raman spectroscopy. *Biochemistry* 49: 3815–3823, 2010.
44. Ignarro LJ. (Ed.) *Nitric Oxide Biology and Pathobiology.* San Diego: Academic Press, 2010.
45. Iyer LM, Anantharaman V, and Aravind L. Ancient conserved domains shared by animal soluble guanylyl cyclases and bacterial signaling proteins. *BMC Genomics* 4: 5, 2003.
46. Jabs A, Oelze M, Mikhed Y, Stamm P, Kroller-Schon S, Welschof P, Jansen T, Hausding M, Kopp M, Steven S, Schulz E, Stasch JP, Munzel T, and Daiber A. Effect of soluble guanylyl cyclase activator and stimulator therapy on nitroglycerin-induced nitrate tolerance in rats. *Vasc Pharmacol* 71: 181–191, 2015.
47. Kazerounian S, Pitari GM, Ruiz-Stewart I, Schulz S, and Waldman SA. Nitric oxide activation of soluble guanylyl cyclase reveals high and low affinity sites that mediate allosteric inhibition by calcium. *Biochemistry* 41: 3396–3404, 2002.
48. Kharitonov VG, Sharma VS, Magde D, and Koesling D. Kinetics and equilibria of soluble guanylate cyclase ligation by CO: effect of YC-1. *Biochemistry* 38: 10699–10706, 1999.
49. Ko FN, Wu CC, Kuo SC, Lee FY, and Teng CM. YC-1, a novel activator of platelet guanylate cyclase. *Blood* 84: 4226–4233, 1994.
50. Kraehling JR, Busker M, Haase T, Haase N, Koglin M, Linnenbaum M, and Behrends S. The amino-terminus of nitric oxide sensitive guanylyl cyclase alpha(1) does not affect dimerization but influences subcellular localization. *PLoS One* 6: e25772, 2011.
51. Lamothe M, Chang FJ, Balashova N, Shirokov R, and Beuve A. Functional characterization of nitric oxide and YC-1 activation of soluble guanylyl cyclase: structural implication for the YC-1 binding site? *Biochemistry* 43: 3039–3048, 2004.
52. Li H and Poulos TL. Structure-function studies on nitric oxide synthases. *J Inorg Biochem* 99: 293–305, 2005.
53. Li Z, Pal B, Takenaka S, Tsuyama S, and Kitagawa T. Resonance Raman evidence for the presence of two heme pocket conformations with varied activities in CO-bound bovine soluble guanylate cyclase and their conversion. *Biochemistry* 44: 939–946, 2005.
54. Ma X, Beuve A, and van den Akker F. Crystal structure of the signaling helix coiled-coil domain of the beta1 subunit of the soluble guanylyl cyclase. *BMC Struct Biol* 10: 2, 2010.
55. Ma X, Sayed N, Baskaran P, Beuve A, and van den Akker F. PAS-mediated dimerization of soluble guanylyl cyclase revealed by signal transduction histidine kinase domain crystal structure. *J Biol Chem* 283: 1167–1178, 2008.
56. Makino R, Park SY, Obayashi E, Iizuka T, Hori H, and Shiro Y. Oxygen binding and redox properties of the heme in soluble guanylate cyclase: implications for the mechanism of ligand discrimination. *J Biol Chem* 286: 15678–15687, 2011.
57. Makino R, Yazawa S, Hori H, and Shiro Y. Interactions of soluble guanylate cyclase with a P-site inhibitor: effects of gaseous heme ligands, azide, and allosteric activators on the binding of 2′-deoxy-3′-GMP. *Biochemistry* 51: 9277–9289, 2012.
58. Martin E, Berka V, Bogatenkova E, Murad F, and Tsai AL. Ligand selectivity of soluble guanylyl cyclase: effect

of the hydrogen-bonding tyrosine in the distal heme pocket on binding of oxygen, nitric oxide, and carbon monoxide. *J Biol Chem* 281: 27836–27845, 2006.
59. Martin E, Czarnecki K, Jayaraman V, Murad F, and Kincaid J. Resonance Raman and infrared spectroscopic studies of high-output forms of human soluble guanylyl cyclase. *J Am Chem Soc* 127: 4625–4631, 2005.
60. Martin E, Golunski E, Laing ST, Estrera AL, and Sharina IG. Alternative splicing impairs soluble guanylyl cyclase function in aortic aneurysm. *Am J Physiol Heart Circ Physiol* 307: H1565–H1575, 2014.
61. Martin F, Baskaran P, Ma X, Dunten PW, Schaefer M, Stasch JP, Beuve A, and van den Akker F. Structure of cinaciguat (BAY 58–2667) bound to Nostoc H-NOX domain reveals insights into heme-mimetic activation of the soluble guanylyl cyclase. *J Biol Chem* 285: 22651–22657, 2010.
62. Mathis KJ, Emmons TL, Curran DF, Day JE, and Tomasselli AG. High yield purification of soluble guanylate cyclase from bovine lung. *Protein Expr Purif* 60: 58–63, 2008.
63. Meurer S, Pioch S, Pabst T, Opitz N, Schmidt PM, Beckhaus T, Wagner K, Matt S, Gegenbauer K, Geschka S, Karas M, Stasch JP, Schmidt HH, and Muller-Esterl W. Nitric oxide-independent vasodilator rescues heme-oxidized soluble guanylate cyclase from proteasomal degradation. *Circ Res* 105: 33–41, 2009.
64. Mittendorf J, Weigand S, Alonso-Alija C, Bischoff E, Feurer A, Gerisch M, Kern A, Knorr A, Lang D, Muenter K, Radtke M, Schirok H, Schlemmer KH, Stahl E, Straub A, Wunder F, and Stasch JP. Discovery of riociguat (BAY 63–2521): a potent, oral stimulator of soluble guanylate cyclase for the treatment of pulmonary hypertension. *ChemMedChem* 4: 853–865, 2009.
65. Moglich A, Ayers RA, and Moffat K. Structure and signaling mechanism of Per-ARNT-Sim domains. *Structure* 17: 1282–1294, 2009.
66. Montfort WR, Weichsel A, and Andersen JF. Nitrophorins and related antihemostatic lipocalins from *Rhodnius prolixus* and other blood-sucking arthropods. *Biochim Biophys Acta* 1482: 110–118, 2000.
67. Morton DB and Vermehren A. Soluble guanylyl cyclases in invertebrates: targets for NO and O(2). *Adv Exp Biol* 1: 65–82, 2007.
68. Mota F, Allerston CK, Hampden-Smith K, Garthwaite J, and Selwood DL. Surface plasmon resonance using the catalytic domain of soluble guanylate cyclase allows the detection of enzyme activators. *Bioorg Med Chem Lett* 24: 1075–1079, 2014.
69. Mou TC, Masada N, Cooper DM, and Sprang SR. Structural basis for inhibition of mammalian adenylyl cyclase by calcium. *Biochemistry* 48: 3387–3397, 2009.
70. Muralidharan S and Boon EM. Heme flattening is sufficient for signal transduction in the H-NOX family. *J Am Chem Soc* 134: 2044–2046, 2012.
71. Murrell W. Nitro-glycerine as a remedy for angina pectoris. *Lancet* 113: 113–115, 1879.
72. Nighorn A, Gibson NJ, Rivers DM, Hildebrand JG, and Morton DB. The nitric oxide-cGMP pathway may mediate communication between sensory afferents and projection neurons in the antennal lobe of *Manduca sexta*. *J Neurosci* 18: 7244–7255, 1998.
73. Nioche P, Berka V, Vipond J, Minton N, Tsai AL, and Raman CS. Femtomolar sensitivity of a NO sensor from *Clostridium botulinum*. *Science* 306: 1550–1553, 2004.
74. Olea C, Boon EM, Pellicena P, Kuriyan J, and Marletta MA. Probing the function of heme distortion in the H-NOX family. *ACS Chem Biol* 3: 703–710, 2008.
75. Olea C, Jr., Kuriyan J, and Marletta MA. Modulating heme redox potential through protein-induced porphyrin distortion. *J Am Chem Soc* 132: 12794–12795, 2010.
76. Pal B, Tanaka K, Takenaka S, and Kitagawa T. Resonance Raman spectroscopic investigation of structural changes of CO-heme in soluble guanylate cyclase generated by effectors and substrate. *J Raman Spectrosc* 41: 1178–1184, 2010.
77. Papapetropoulos A, Hobbs AJ, and Topouzis S. Extending the translational potential of targeting NO/cGMP-regulated pathways in the CVS. *Br J Pharmacol* 172: 1397–1414, 2015.
78. Pellicena P, Karow DS, Boon EM, Marletta MA, and Kuriyan J. Crystal structure of an oxygen-binding heme domain related to soluble guanylate cyclases. *Proc Natl Acad Sci U S A* 101: 12854–12859, 2004.
79. Persson A, Gross E, Laurent P, Busch KE, Bretes H, and de Bono M. Natural variation in a neural globin tunes oxygen sensing in wild *Caenorhabditis elegans*. *Nature* 458: 1030–1033, 2009.
80. Purohit R, Fritz BG, The J, Issaian A, Weichsel A, David CL, Campbell E, Hausrath AC, Rassouli-Taylor L, Garcin ED, Gage MJ, and Montfort WR. YC-1 Binding to the beta subunit of soluble guanylyl cyclase overcomes allosteric inhibition by the alpha subunit. *Biochemistry* 53: 101–114, 2014.
81. Purohit R, Weichsel A, and Montfort WR. Crystal structure of the alpha subunit PAS domain from soluble guanylyl cyclase. *Protein Sci* 22: 1439–1444, 2013.
82. Ramanathan S, Mazzalupo S, Boitano S, and Montfort WR. Thrombospondin-1 and angiotensin II inhibit soluble guanylyl cyclase through an increase in intracellular calcium concentration. *Biochemistry* 50: 7787–7799, 2011.
83. Ribeiro JMC, Hazzard JMH, Nussenzveig RH, Champagne DE, and Walker FA. Reversible binding of nitric oxide by a salivary heme protein from a bloodsucking insect. *Science* 260: 539–541, 1993.
84. Roberts LR, Bradley PA, Bunnage ME, England KS, Fairman D, Fobian YM, Fox DN, Gymer GE, Heasley SE, Molette J, Smith GL, Schmidt MA, Tones MA, and Dack KN. Acidic triazoles as soluble guanylate cyclase stimulators. *Bioorg Med Chem Lett* 21: 6515–6518, 2011.
85. Roberts SA, Weichsel A, Qiu Y, Shelnutt JA, Walker FA, and Montfort WR. Ligand-induced heme ruffling and bent NO geometry in ultra-high resolution structures of nitrophorin 4. *Biochemistry* 40: 11327–11337, 2001.
86. Rose EJ and Hoffman BM. Nitric-oxide ferrohemes—kinetics of formation and photo-dissociation quantum yields. *J Am Chem Soc* 105: 2866–2873, 1983.
87. Roy B, Halvey EJ, and Garthwaite J. An enzyme-linked receptor mechanism for nitric oxide-activated guanylyl cyclase. *J Biol Chem* 283: 18841–18851, 2008.
88. Ruiz-Stewart I, Tiyyagura SR, Lin JE, Kazerounian S, Pitari GM, Schulz S, Martin E, Murad F, and Waldman SA. Guanylyl cyclase is an ATP sensor coupling nitric oxide signaling to cell metabolism. *Proc Natl Acad Sci U S A* 101: 37–42, 2004.
89. Russwurm M and Koesling D. NO activation of guanylyl cyclase. *EMBO J* 23: 4443–4450, 2004.
90. Sarkar A, Dai Y, Haque MM, Seeger F, Ghosh A, Garcin ED, Montfort WR, Hazen SL, Misra S, and Stuehr DJ. Heat shock protein 90 associates with the Per-Arnt-Sim domain

of heme-free soluble guanylate cyclase: implications for enzyme maturation. *J Biol Chem* 290: 21615–21628, 2015.
91. Schaap P. Guanylyl cyclases across the tree of life. *Front Biosci* 10: 1485–1498, 2005.
92. Schindler U, Strobel H, Schonafinger K, Linz W, Lohn M, Martorana PA, Rutten H, Schindler PW, Busch AE, Sohn M, Topfer A, Pistorius A, Jannek C, and Mulsch A. Biochemistry and pharmacology of novel anthranilic acid derivatives activating heme-oxidized soluble guanylyl cyclase. *Mol Pharmacol* 69: 1260–1268, 2006.
93. Schmidt PM, Schramm M, Schroder H, Wunder F, and Stasch JP. Identification of residues crucially involved in the binding of the heme moiety of soluble guanylate cyclase. *J Biol Chem* 279: 3025–3032, 2004.
94. Seeger F, Quintyn R, Tanimoto A, Williams GJ, Tainer JA, Wysocki VH, and Garcin ED. Interfacial residues promote an optimal alignment of the catalytic center in human soluble guanylate cyclase: heterodimerization is required but not sufficient for activity. *Biochemistry* 53: 2153–2165, 2014.
95. Serfass L, Carr HS, Aschenbrenner LM, and Burstyn JN. Calcium ion downregulates soluble guanylyl cyclase activity: evidence for a two-metal ion catalytic mechanism. *Arch Biochem Biophys* 387: 47–56, 2001.
96. Sharina IG, Jelen F, Bogatenkova EP, Thomas A, Martin E, and Murad F. Alpha1 soluble guanylyl cyclase (sGC) splice forms as potential regulators of human sGC activity. *J Biol Chem* 283: 15104–15113, 2008.
97. Shelnutt JA, Song X-Z, Ma J-G, Jia S-L, Jentzen W, and Medforth CJ. Nonplanar porphyrins and their significance in proteins. *Chem Soc Rev* 27: 31–41, 1998.
98. Shi R, McDonald L, Cygler M, and Ekiel I. Coiled-coil helix rotation selects repressing or activating state of transcriptional regulator DhaR. *Structure* 22: 478–487, 2014.
99. Shokhireva T, Berry RE, Uno E, Balfour CA, Zhang H, and Walker FA. Electrochemical and NMR spectroscopic studies of distal pocket mutants of nitrophorin 2: stability, structure, and dynamics of axial ligand complexes. *Proc Natl Acad Sci U S A* 100: 3778–3783, 2003.
100. Sinha SC and Sprang SR. Structures, mechanism, regulation and evolution of class III nucleotidyl cyclases. *Rev Physiol Biochem Pharmacol* 157: 105–140, 2006.
101. Stasch J-P, Becker EM, Alonso-Alija C, Apeler H, Gerzer R, Minuth T, Perzborn E, Pleiss U, Schröder H, Schroeder W, Stahl E, Steinke W, Straub A, and Schramm M. NO-independent regulatory site on soluble guanylate cyclase. *Nature* 410: 212–215, 2001.
102. Stone JR and Marletta MA. Soluble guanylate cyclase from bovine lung: activation with nitric oxide and carbon monoxide and spectral characterization of the ferrous and ferric states. *Biochemistry* 33: 5636–5640, 1994.
103. Stone JR and Marletta MA. Spectral and kinetic studies on the activation of soluble guanylate cyclase by nitric oxide. *Biochemistry* 35: 1093–1099, 1996.
104. Stone JR and Marletta MA. Synergistic activation of soluble guanylate cyclase by YC-1 and carbon monoxide: implications for the role of cleavage of the iron-histidine bond during activation by nitric oxide. *Chem Biol* 5: 255–261, 1998.
105. Stuehr DJ, Tejero J, and Haque MM. Structural and mechanistic aspects of flavoproteins: electron transfer through the nitric oxide synthase flavoprotein domain. *FEBS J* 276: 3959–3974, 2009.
106. Surmeli NB, Muskens FM, and Marletta MA. The influence of nitric oxide on soluble guanylate cyclase regulation by nucleotides: role of the pseudosymmetric site. *J Biol Chem* 290: 15570–15580, 2015.
107. Tesmer JJ, Sunahara RK, Gilman AG, and Sprang SR. Crystal structure of the catalytic domains of adenylyl cyclase in a complex with Gsalpha.GTPgammaS. *Science* 278: 1907–1916, 1997.
108. Traylor TG and Sharma VS. Why NO? *Biochemistry* 31: 2847–2849, 1992.
109. Tsai AL, Berka V, Martin E, and Olson JS. A ''sliding scale rule'' for selectivity among NO, CO, and O(2) by heme protein sensors. *Biochemistry* 51: 172–186, 2012.
110. Tsai AL, Berka V, Sharina I, and Martin E. Dynamic ligand exchange in soluble guanylyl cyclase (sGC): implications for sGC regulation and desensitization. *J Biol Chem* 286: 43182–43192, 2011.
111. Tsai AL, Martin E, Berka V, and Olson JS. How do heme-protein sensors exclude oxygen? Lessons learned from cytochrome c′, Nostoc puntiforme heme nitric oxide/oxygen-binding domain, and soluble guanylyl cyclase. *Antioxid Redox Signal* 17: 1246–1263, 2012.
112. Underbakke ES, Iavarone AT, Chalmers MJ, Pascal BD, Novick S, Griffin PR, and Marletta MA. Nitric oxide-induced conformational changes in soluble guanylate cyclase. *Structure* 22: 602–611, 2014.
113. Underbakke ES, Iavarone AT, and Marletta MA. Higher-order interactions bridge the nitric oxide receptor and catalytic domains of soluble guanylate cyclase. *Proc Natl Acad Sci U S A* 110: 6777–6782, 2013.
114. Waldman SA and Murad F. Cyclic GMP synthesis and function. *Pharmacol Rev* 39: 163–196, 1987.
115. Walker FA. Nitric oxide interaction with insect nitrophorins and thoughts on the electron configuration of the {FeNO}6 complex. *J Inorg Biochem* 99: 216–236, 2005.
116. Wedel B, Humbert P, Harteneck C, Foerster J, Malkewitz J, Böhme E, Schultz G, and Koesling D. Mutation of His-105 in the b1 subunit yields a nitric oxide-insensitive form of soluble guanylate cyclase. *Proc Natl Acad Sci U S A* 91: 2592–2596, 1994.
117. Weichsel A, Andersen JF, Roberts SA, and Montfort WR. Reversible nitric oxide binding to nitrophorin 4 from *Rhodnius prolixus* involves complete distal pocket burial. *Nat Struct Biol* 7: 551–554, 2000.
118. Weichsel A, Maes EM, Andersen JF, Valenzuela JG, Shokhireva T, Walker FA, and Montfort WR. Heme-assisted S-nitrosation of a proximal thiolate in a nitric oxide transport protein. *Proc Natl Acad Sci U S A* 102: 594–599, 2005.
119. Winger JA, Derbyshire ER, Lamers MH, Marletta MA, and Kuriyan J. The crystal structure of the catalytic domain of a eukaryotic guanylate cyclase. *BMC Struct Biol* 8: 42, 2008.
120. Wood KC, Batchelor AM, Bartus K, Harris KL, Garthwaite G, Vernon J, and Garthwaite J. Picomolar nitric oxide signals from central neurons recorded using ultrasensitive detector cells. *J Biol Chem* 286: 43172–43181, 2011.
121. Yazawa S, Tsuchiya H, Hori H, and Makino R. Functional characterization of two nucleotide-binding sites in soluble guanylate cyclase. *J Biol Chem* 281: 21763–21770, 2006.
122. Yoo BK, Lamarre I, Martin JL, and Negrerie M. Quaternary structure controls ligand dynamics in soluble guanylate cyclase. *J Biol Chem* 287: 6851–6859, 2012.
123. Yoo BK, Lamarre I, Martin JL, Rappaport F, and Negrerie M. Motion of proximal histidine and structural allosteric transition in soluble guanylate cyclase. *Proc Natl Acad Sci U S A* 112: E1697–E1704, 2015.

124. Yoo BK, Lamarre I, Rappaport F, Nioche P, Raman CS, Martin JL, and Negrerie M. Picosecond to second dynamics reveals a structural transition in *Clostridium botulinum* NO-sensor triggered by the activator BAY-41–2272. *ACS Chem Biol* 7: 2046–2054, 2012.
125. Zhang G, Liu Y, Ruoho AE, and Hurley JH. Structure of the adenylyl cyclase catalytic core. *Nature* 386: 247–253, 1997.
126. Zhao Y, Brandish PE, Ballou DP, and Marletta MA. A molecular basis for nitric oxide sensing by soluble guanylate cyclase. *Proc Natl Acad Sci U S A* 96: 14753–14758, 1999.
127. Zhou Z, Sayed N, Pyriochou A, Roussos C, Fulton D, Beuve A, and Papapetropoulos A. Protein kinase G phosphorylates soluble guanylyl cyclase on serine 64 and inhibits its activity. *Arterioscler Thromb Vasc Biol* 28: 1803–1810, 2008.
128. Zimmer M, Gray JM, Pokala N, Chang AJ, Karow DS, Marletta MA, Hudson ML, Morton DB, Chronis N, and Bargmann CI. Neurons detect increases and decreases in oxygen levels using distinct guanylate cyclases. *Neuron* 61: 865–879, 2009.

Address correspondence to:
Dr. William R. Montfort
Department of Chemistry and Biochemistry
University of Arizona
Tucson, AZ 85721

E-mail: montfort@email.arizona.edu

Date of first submission to ARS Central, March 13, 2016; date of acceptance, March 15, 2016.

Abbreviations Used

AUC = analytical ultracentrifugation
CC = coiled coil
CFP = cyan fluorescent protein
cGMP = guanosine 3′,5′-cyclic monophosphate
CHD = cyclase homology domain
EM = electron microscopy
FRET = Förster resonance energy transfer
HNOB = heme NO binding
H-NOX domain = heme-nitric oxide/oxygen binding domain
hsp90 = heat shock protein 90
Ms sGC = *Manduca sexta* sGC
NO = nitric oxide
PAS domain = Per-ARNT-Sim domain
PKG = protein kinase G
SAXS = small-angle X-ray scattering
sGC = soluble guanylyl/guanylate cyclase
SONO = sensor of nitric oxide
SPR = surface plasmon resonance
STHK = signal transduction histidine kinase
YFP = yellow fluorescent protein